

## Article

# Small Punch Test to Estimate the Threshold Stress in Aggressive Environments by Incremental Step Loading

Borja Arroyo <sup>1,2,\*</sup>, Laura Andrea <sup>1</sup>, José A. Álvarez <sup>1</sup>, Sergio Cicero <sup>1,\*</sup>, Federico Gutiérrez-Solana <sup>1</sup> and Luis Abarca <sup>1</sup>

<sup>1</sup> Departmennt de Ciencia e Ing. del Terreno y de los Materiales, Universidad de Cantabria (LADICIM), E.T.S. de Ing. de Caminos, Canales y Puertos, Av./Los Castros 44, 39005 Santander, Spain; laura.andrea@alumnos.unican.es (L.A.); alvareja@unican.es (J.A.Á.); gsolana@unican.es (F.G.-S.); luis.abarca@alumnos.unican.es (L.A.)

<sup>2</sup> Departmennt de Ing. Geografica y Tecnicas de Expresion Grafica, Universidad de Cantabria, E.T.S. de Ing. de Caminos, Canales y Puertos, Av./Los Castros 44, 39005 Santander, Spain

\* Correspondence: arroyob@unican.es (B.A.); ciceros@unican.es (S.C.)

**Abstract:** The present work is a relevant advance in the validation of the incremental step loading technique (ASTM F1624 standard) when applied to Small Punch tests (SPT) for the threshold load determination of medium- and high-strength steels in aggressive environments, as a novel alternative to conventional time-consuming tests under constant load. It completes previous works by the authors on this topic, extending a methodology to estimate the threshold stress from SPT tests in aggressive environments, covering the whole range of hardness marked by ASTM F1624 as the main goal. This is achieved by calibrating a model of the material's hardness by the use of a coefficient in function of it. For this purpose, four medium- and high-strength steels of 33, 35, 50 and 60 HRC (Hardness Rockwell C) are exposed to three different cathodic polarization hydrogen embrittlement environments of 1, 5 and 10 mA/cm<sup>2</sup> in 1N H<sub>2</sub>SO<sub>4</sub> acid electrolyte connected to a platinum anode. Threshold stresses in these circumstances are obtained by uniaxial specimens following ASTM F1624 and compared to their homologous threshold loads obtained by Small Punch tests according to the authors' original methodology proposal. Finally, the aforementioned model, consisting of a correlation based on composing an elastic and a plastic part, is calibrated for a hardness ranging 33–60 HRC, this being the main original contribution of this work; the elastic part is dependent just on the elastic-to-plastic transition SPT load, while the plastic part is ruled by a material hardness-dependent coefficient. This technique supposes an advance in engineering tools, due to its applicability in situations of material shortage, such as in-service components, welded joints, local areas, complex geometries, small thicknesses, etc., often present in aerospace, automotive or oil-gas, among others.

**Keywords:** threshold stress; small punch test; incremental step loading technique; aggressive environment; medium and high strength steels; hydrogen embrittlement



**Citation:** Arroyo, B.; Andrea, L.; Álvarez, J.A.; Cicero, S.; Gutiérrez-Solana, F.; Abarca, L. Small Punch Test to Estimate the Threshold Stress in Aggressive Environments by Incremental Step Loading. *Metals* **2024**, *14*, 1234. <https://doi.org/10.3390/met14111234>

Academic Editor: Riccardo Nobile

Received: 6 September 2024

Revised: 19 October 2024

Accepted: 26 October 2024

Published: 29 October 2024



**Copyright:** © 2024 by the authors. Licensee MDPI, Basel, Switzerland. This article is an open access article distributed under the terms and conditions of the Creative Commons Attribution (CC BY) license (<https://creativecommons.org/licenses/by/4.0/>).

## 1. Introduction

The mechanical properties of high-strength low-alloy steels have made them very attractive and interesting materials to highly demanding industries, such as aerospace, automotive or oil-gas, continuously increasing their range of applications. One of their few disadvantages, though, is their susceptibility to stress corrosion cracking and hydrogen embrittlement when exposed to harsh environments, which are relatively frequent in such industrial applications. Some well-known examples are gas transport, where H<sub>2</sub>S is considerably present, or offshore applications where cathodic polarization is produced, inducing hydrogen in the steel.

A derived issue is that standardized tests used to characterize materials under aggressive environments [1,2] require a certain number of samples to be tested and slow strain rate tests in the environment, in order to obtain the threshold stress, which means a certain

amount of material and time. Besides the intrinsic inaccuracy of these methods, 10 to 12 specimens are usually required, achieving more than 10,000 h per test [1,2].

To solve this time-consuming issue, the methodology presented in the ASTM F1624 standard [3] was derived. It consists of the application of certain sequences of constant loads that are incremented by timed steps until the specimen fails, which is caused by the combined action of the aggressive environment and the slow solicitation caused by load increments. With this method, the threshold stress,  $\sigma_{thr}$ , can be determined in a few days, testing a minimum of three uniaxial specimens.

In respect to material shortages, there are situations where it is not possible to obtain specimens according to conventional standards, such as in-service components, welded joints, local areas, complex geometries, small thicknesses, etc. For these situations, the Small Punch test (SPT) has been positioned as an alternative [4] in the last decade, being ruled so by the EN 10371 [5] and ASTM E3205 [6] standards, but none of them consider characterization in aggressive environments. In the last decade, the authors have proved that the Small Punch test technique can be employed in environmental-assisted cracking scenarios.

In recent works [7], a preliminary proposal to estimate the threshold load in aggressive environments, based on an adaptation of the ASTM F1624 methodology to Small Punch tests, was presented. However, this proposal was just based on tests with steels of 33–35 HRC (the lowest value of ASTM F1624), so its validity needed to be extended to higher hardness ranges. Also, the step times first employed had been chosen for convenience but needed to be optimized, which was done in [8] by the authors.

The present work extends and validates the proposed incremental SPT step methodology to all ranges of steels hardness over 33 HRC (up to 60 HRC). It goes deeper into the model that estimates the threshold stress from the SPT threshold load, presented in [7], incorporating the optimization of step times from [8]. The ultimate advance achieved in this paper is the calibration of this model, proving that it allows one to obtain the threshold stress based (solely) on SPT tests, with limited experimental scatter (below 10%), and based on both an elastic part depending on the elastic-to-plastic transition SPT load and a plastic part ruled by a material hardness-dependent coefficient, which is calibrated.

## 2. Materials and Methods

### 2.1. Materials

Four steels have been used in this research. On the one hand, an X80 rolled steel [9], commonly used in gas and petroleum low-temperature transportation, with a hardness of 35 HRC, and an S420 weldable thermomechanically treated steel [10] of 33 HRC, used in pressure vessels, power plants and offshore structures. On the other hand, two commercial Uddeholm Arne tool steels of 50 HRC and 60 HRC, hardened both by quenching and tempering. The first two steels have a ferritic–pearlitic microstructure, with grain sizes ranging 5–15  $\mu\text{m}$  for X80 and 5–25  $\mu\text{m}$  for S420, whereas the last two steels have a tempered martensitic microstructure, with grain sizes ranging 5–10  $\mu\text{m}$  in both cases, all of which are shown in Figure 1. The chemical compositions of the four steels are presented in Table 1, obtained by means of spark emission spectrometry, and their mechanical properties are gathered in Table 2, which were derived from  $\phi 10$  mm cylindrical tensile test specimens.

**Table 1.** Chemical composition of the four steels analyzed (weight %).

	C	Si	S	P	Mn	Ni	Cr	Mo	Cu	Al	V	Ti	Nb	W
X80	0.070	0.180	<0.005	<0.005	1.830	0.030	-	0.150	0.020	0.030	-	-	0.030	-
S420	0.080	0.280	0.001	0.012	1.440	0.030	0.030	0.003	0.015	0.026	0.005	0.015	0.031	-
50 HRC	0.947	0.310	<0.035	<0.005	1.093	-	0.614	-	-	-	0.113	-	-	0.598
60 HRC	0.951	0.300	<0.035	<0.005	1.013	-	0.599	-	-	-	0.109	-	-	0.611

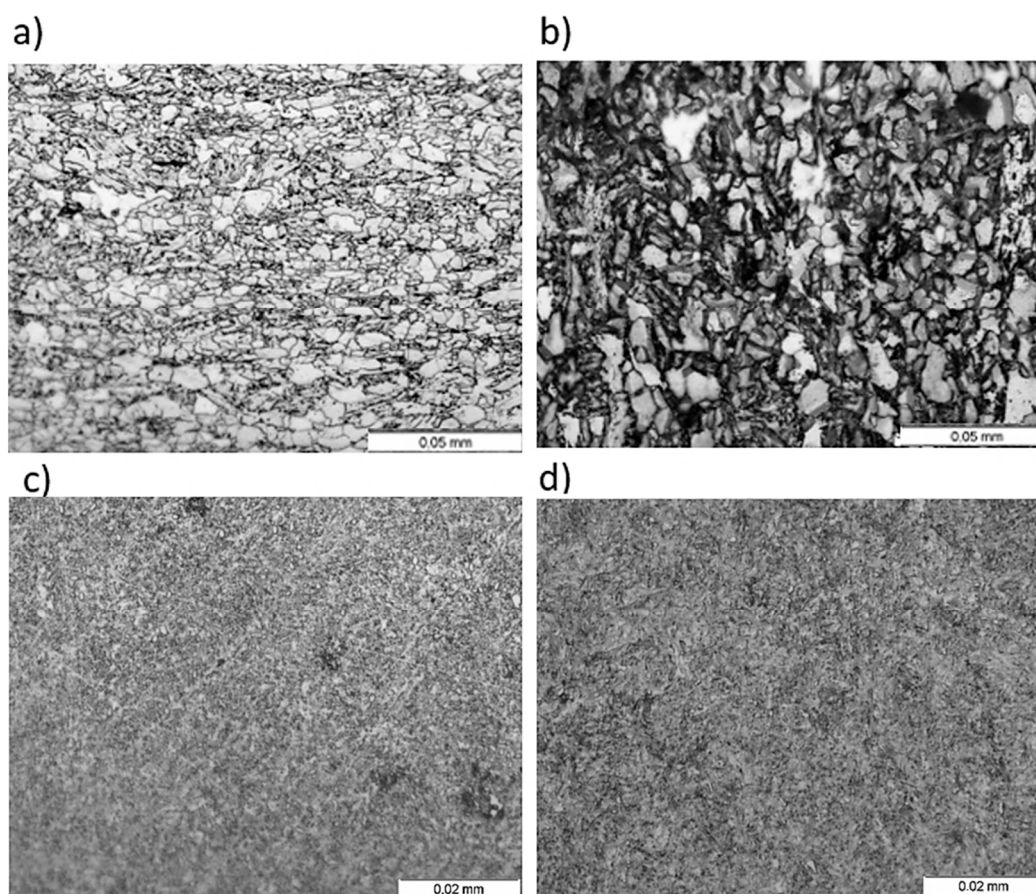


**Figure 1.** Microstructure of: (a) X80 steel, ferritic–pearlitic; (b) S420 steel, ferritic–pearlitic; (c) 50 HRC steel, tempered martensite; (d) 60 HRC steel, tempered martensite.

**Table 2.** Mechanical properties of the four steels analyzed.

	E (GPa)	$\sigma_y$ (MPa)	$\sigma_u$ (MPa)	$e_u$ (%)
X80	209.9	621.3	692.9	29.6
S420	206.4	447.7	547.1	21.7
50 HRC	216.6	1810.7	1935.9	3.1
60 HRC	190.8	929.8	1995.5	1.9

## 2.2. Aggressive Environments

In order to obtain a proper material characterization under Hydrogen-Induced Cracking (HIC) [11] conditions, a simulated hydrogen environment is used in this work, also providing a cathodic polarization of the specimens [12]. In order to achieve different hydrogen absorption levels, and therefore to simulate different levels of environment aggressiveness, the intensity of the electric current applied during the cathodic polarization [13] was fixed at 1, 5 and 10 mA/cm<sup>2</sup>. The electrolyte used was a 1 N H<sub>2</sub>SO<sub>4</sub> solution in distilled water, containing 10 mg of As<sub>2</sub>O<sub>3</sub>, prepared according to Pressouyre’s method [14] and with 10 drops of CS<sub>2</sub> per liter, the final acid pH being between 0.65 and 0.80. The specimen works as an electrode, platinum as a counter electrode and a saturated calomel electrode as the reference electrode, and the tests are performed at room temperature (20 ± 2 °C), with continuous water agitation to remove hydrogen bubbles from the specimen surface and, thus, avoiding local corrosion deposits [1]; this was accomplished by blowing air through a pipe placed in the bottom of the electrolytic cell at 6 bar pressure to make the liquid moving.

### 2.3. Tensile Tests According to ASTM F1624 [3]

The target of these tests is to determine the threshold load ( $P_{th}$ ) and the corresponding threshold stress ( $\sigma_{th}$ ), following the standard ASTM F1624 [3]. With this purpose, tensile cylindrical specimens were machined [15] with a central diameter of 6 mm, while the area to be tested was completely immersed in the solution. Special care must be taken to locate the specimen in the electrolytic cell, assuring an electrical isolation of the specimen while keeping the cell's tightness. Before starting the mechanical step loading, the specimens were previously exposed to the same embrittling environment over 24 h to assure a proper hydrogen distribution [14]. Based on the steel hardness, the load step protocol to be applied is defined in Table 3, with the experimental setup being shown in Figure 2.

**Table 3.** Step load profiles according to ASTM F1624 [3].

Hardness	Step	Step Load	Step Time (h)	Profile Code [3]
$33 \leq \text{HRC} < 45$	1–10	5% of $P_{FFL}$	2	(10/5/2,4)
	11–20		4	
$45 \leq \text{HRC} < 55$	1–10	5% of $P_{FFL}$	1	(10/5/1,2)
	11–20		2	
$\geq 55$	1–20	5% of $P_{FFL}$	1	(10/5/1)

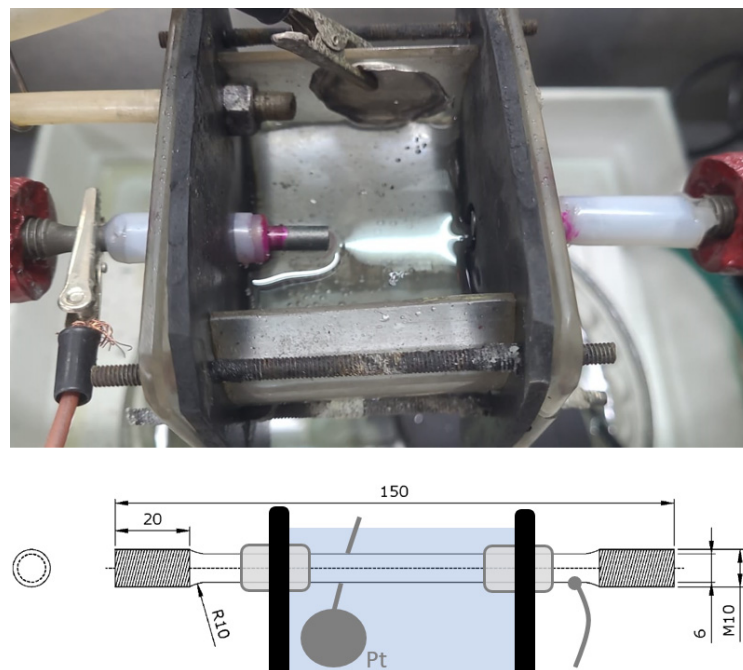


**Figure 2.** General view just after specimen failure (**up**) and schematic (**bottom**) of the experimental setup for ASTM F1624 step load profiles.

ASTM F1624 [3] indicates the following procedure to be followed to determine the threshold, as shown in Figure 3: as a first step, a tensile test is performed in air according to [15] to obtain the Fast Fracture Load ( $P_{FFL}$ ). Next, the step protocol is defined with 20 step sequences of  $P_{FFL}/20$  load value each step, until the sample failure is reached, which gives the  $P_{th-1}$  load value (see Table 3 for step durations in function of the steel hardness according ASTM F1624). The following step sequences, designed with a load for the 20th step obtained by increasing the threshold load of the previous sequence by 10%, provides the values for  $P_{th-2}$ ,  $P_{th-3}$ , . . .  $P_{th-n}$ , respectively. With a minimum of 3 sequences, the final threshold load is obtained as soon as the difference between two consecutive sequence threshold loads is below 5% (the load corresponding to one step). This is to

allow the environment to produce its embrittling effect close to the threshold in the areas of the specimen under plasticization, due to the lower solicitation rates at the last steps when compared to those at the initial steps (where the process is governed by elasticity instead). Note that in the highest hardness range from Table 3,  $HRC \geq 55$ , all 20 steps last the same, this usually being the case with very high-strength steels, which are more affected by aggressive environments [16].

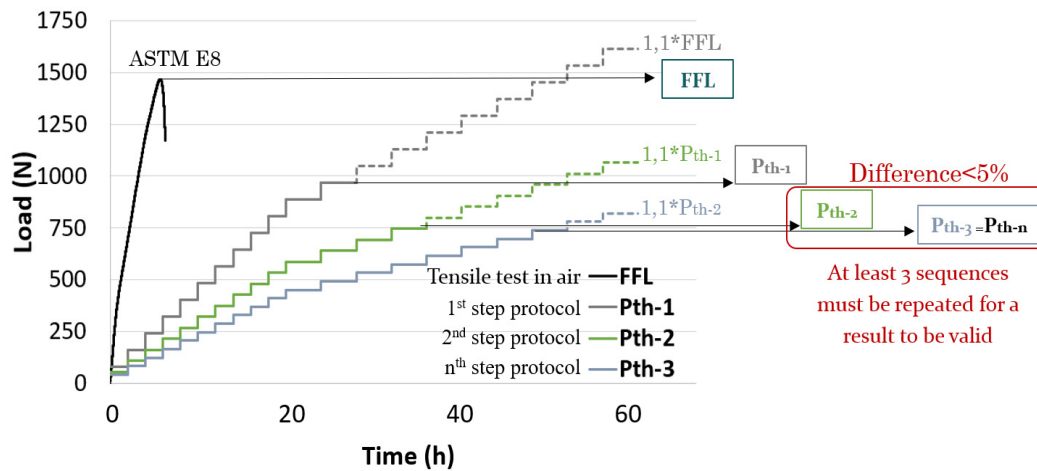


**Figure 3.** Schematic of the ASTM-F1624 methodology for a  $33 \leq HRC < 45$  steel.

#### 2.4. Small Punch Test (SPT) Main Concepts

The SPT is a quasi-non-destructive test, since the extraction of the small amount of material required does not compromise the component's integrity, allowing one to test in-service materials (repairing the sampling hollows). It was firstly developed in the 1980s, and nowadays it has become a worldwide alternative for the estimation of mechanical properties when it is not possible to obtain specimens that fit regular standards; both European [5] and American [6] standards have been published, covering tensile, creep and fracture properties estimations.

The SPT consists of punching a plane specimen (0.5 mm nominal thickness and less than  $1 \text{ cm}^2$  cross-section), deforming it until it breaks. Figure 4 shows the device used for the performance of the tests in this work, according to the European standard [5].

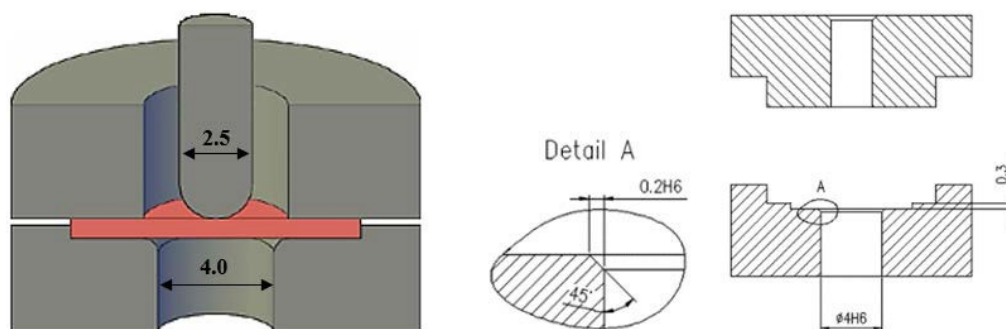


**Figure 4.** Small Punch test experimental device used in this work (left), including the recommendations of the European standard [5]; dimensions in mm.

During the test, the force and the punch displacement are registered continuously, obtaining a curve such as the one presented in Figure 5; the fracture has a semicircular shape (smile-type or cupping type) in ductile scenarios or multi-radial (star-type) shape in brittle ones [5]. The curve can be divided into four main regions: I (plate bending quasi-totally elastic), II (plate bending partially plasticized in the most stressed face of the

specimen), III (membrane stretching) and IV (instability). Two main parameters can be pointed out:

- $P_y$ : elastic-to-plastic load, which marks the beginning of plastics effects on the specimen; this means the end of pure elastic behavior, so the beginning of the plasticity hydrogen-assisted effect; it is identified with the first convexity change in the curve;
- $P_{max}$ : maximum load reached during the test, after which the sample's collapse is imminent. The energy below the test curve,  $E_{SP}$ , is defined up to this load.

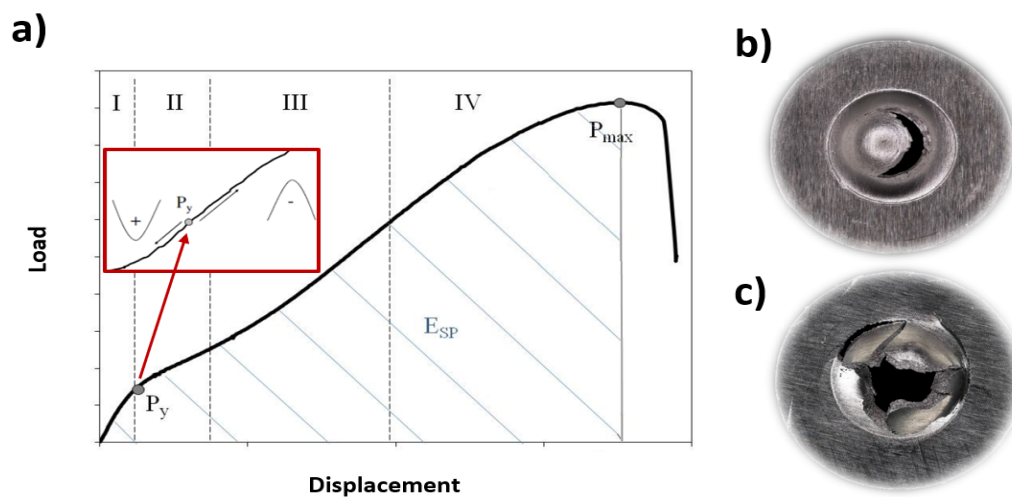


**Figure 5.** (a) Schematic of the SPT load–displacement curve; (b) broken specimen from ductile scenario; (c) broken specimen from brittle scenario.

### 2.5. Application of ASTM F1624 [3] Step Methodology to SPT

The aim of the research carried out in this work, as well as in the previously published works [7,8], has been to apply the incremental step loading technique to SPT as strictly as possible, assuming the necessary adaptations.

SPT specimens are  $10 \times 10 \text{ mm}^2$  square plates with a thickness of  $0.5 \pm 0.01 \text{ mm}$ , according to [5] and as validated in [17]. Therefore, some modifications had to be performed based on the Small Punch's particularities:

- Firstly,  $P_{FFL-SPT}$  is obtained in this case from an SPT test in air according to [5]; this test is also used to derive the elastic-to-plastic load,  $P_y$ , as the first inflexion point of the obtained load–displacement curve, as described in [7];
- Then, given that the diffusion time is proportional to the square of the thickness [18], the SPT specimens must be previously immersed in the environment during less time than that taken by conventional specimens. Two hours was derived to be the most suitable time according the literature [7,8];
- Also, for a similar reason, according to [8], the optimal step times, combining a complete environmental affection with the shortest possible time, were phenomenologically proved to be equal to one-sixth of the durations indicated in the ASTM F1624 standard [8] for each hardness range (Table 3), as presented in Table 4.

**Table 4.** Step load profiles employed in the SPT proposal.

Hardness	Step	Step Load	Step Time (min)
$33 \leq \text{HRC} < 45$	1–10	5% of $P_{FFL-SPT}$	20
	11–20		40
$45 \leq \text{HRC} < 55$	1–10	5% of $P_{FFL-SPT}$	10
	11–20		20
$\geq 55$	1–20	5% of $P_{FFL-SPT}$	10

The device employed is an electrolytic cell in which the SPT sample is embedded into two jigs and punched by the action of the load applied on it, while completely immersed in the solution during the whole test (see Figure 6).

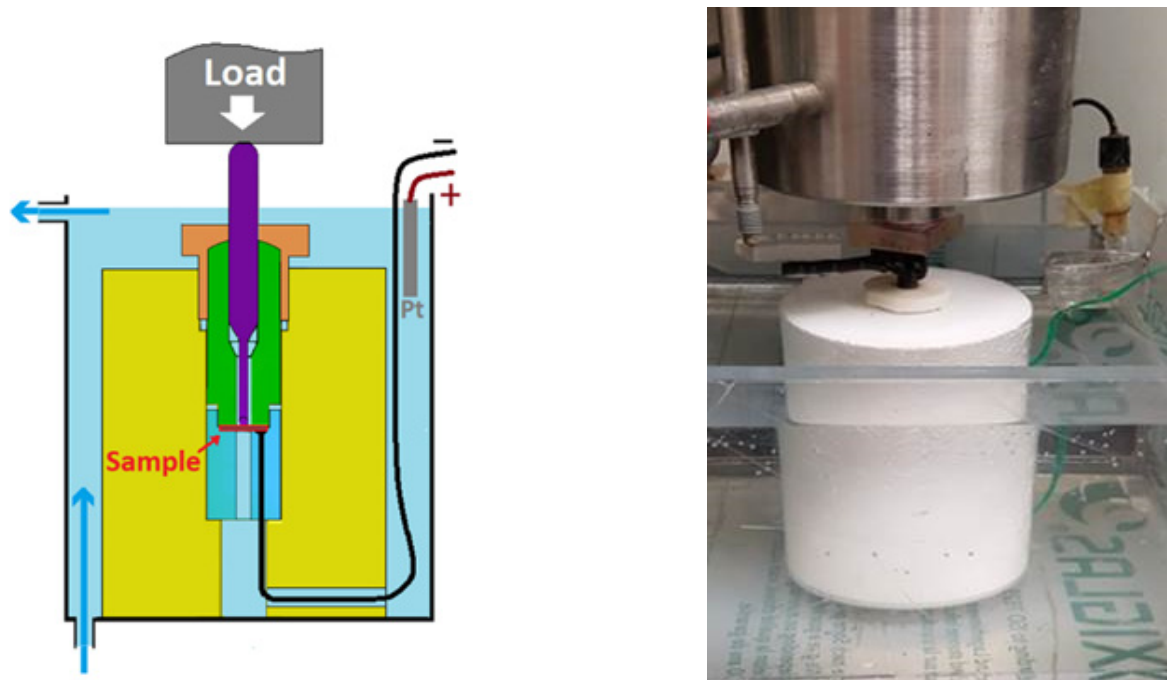


**Figure 6.** Schematic (left) and overview (right) of the testing device for SPT tests.

### 2.6. Estimation of the Threshold Stress ( $\sigma_{th}$ ) Based on the SPT Threshold Load ( $P_{th-SPT}$ )

Based on the proportionality in the threshold stress reduction (uniaxial specimens) and the SPT threshold load reduction, together with the findings shown in the literature, a model to estimate  $\sigma_{th}$  based on  $P_{th-SPT}$  was presented by the authors in [7]. The threshold stress,  $\sigma_{th}$ , derived from the SPT is calculated as the sum of two terms: one elastic ( $\sigma_{el-SPT}$ ), not affected by the environment, and one plastic ( $\sigma_{pl-SPT}$ ), assisted by environment phenomena, which tends to provide the biggest contribution to the final value.

$$\sigma_{th-SPT} = \sigma_{el-SPT} + \sigma_{pl-SPT} \quad (1)$$

The elastic component can be obtained from the elastic-to-plastic load,  $P_y$ , which defines the start of plastic phenomena; it is derived from the SPT test in air, which according to [5] is employed to determine  $P_{FFL}$  (as mentioned in Section 2.3). Then, the elastic part is calculated, based on [19], as the maximum stress in the most stressed face of a circular plate of thickness “ $h_0$ ” embedded around the entire perimeter and subjected to a centered vertical load “ $P_y$ ”, as shown in Equation (2):

$$\sigma_{el-SPT} = \frac{3}{2 \cdot \pi \cdot h_0^2} \cdot P_y \quad (2)$$

The plastic component follows the usual approach in SPT correlations to determine tensile parameters such as yield stress or tensile strength [5,19], consisting of normalizing the load by “ $h_0^2$ ” and employing a correlation coefficient. However, in this case, as proved in previous works [7], just the plastic part of the SPT threshold load ( $P_{th-SPT} - P_y$ ) contributes to its calculation (as  $P_y$  has already been included in the elastic one), resulting in the following expression:

$$\sigma_{pl-SPT} = \frac{\alpha}{h_0^2} \cdot (P_{th-SPT} - P_y) \quad (3)$$

where “ $\alpha$ ” is a dimensionless correlation coefficient, loads are introduced in newtons and “ $h_0$ ” in millimeters. This leads to

$$\sigma_{th-SPT} = \sigma_{el-SPT} + \sigma_{pl-SPT} = \frac{3}{2 \cdot \pi \cdot h_0^2} \cdot P_y + \frac{\alpha}{h_0^2} \cdot (P_{th-SPT} - P_y) \quad (4)$$

### 3. Results

In this section, all the results obtained from the specimens tested by both ASTM F1624 [3] tests with cylindrical specimens and SPT tests according to the proposal presented are collected in Table 5. In it, all the different material and environment combinations and the threshold load values obtained with the proposed SPT method and their corresponding threshold stress counterparts according to ASTM F1624 [3] are presented. Also, the values of  $P_y$  obtained in the SPT in air are included, being necessary for further calculations.

**Table 5.** Results of SPT tests according to the proposal, and tests results on uniaxial specimens according to ASTM F1624 [3].

	P <sub>y</sub> (SPT)		Fast Fracture Load		1 mA/cm <sup>2</sup>		5 mA/cm <sup>2</sup>		10 mA/cm <sup>2</sup>	
	Proposal P <sub>y</sub> (N)	Proposal P <sub>FEL-SPT</sub> (N)	ASTM FFL (MPa)	Proposal P <sub>th-SPT</sub> (N)	ASTM σ <sub>th</sub> (MPa)	Proposal P <sub>th-SPT</sub> (N)	ASTM σ <sub>th</sub> (MPa)	Proposal P <sub>th-SPT</sub> (N)	ASTM σ <sub>th</sub> (MPa)	
X80 (35 HRC)	121	1490	693	943	556	638	446	620	436	
S420 (33 HRC)	69	1465	548	812	379	625	265	594	257	
50 HRC	22	1428	1917	321	337	291	295	257	247	
60 HRC	10	677	1975	182	293	142	185	114	152	

As an example of this, Figure 7 presents the results for 60 HRC steel in the three environments studied (all the test records end up in graphs that lead to the same numerical values of Table 5 but with less quality). On the left, the threshold stresses’ step protocols according to ASTM F1624 are presented, while on the right their corresponding threshold load values obtained with the proposed SPT method can be found. The results are organized in rows, an environment of 1 mA/cm<sup>2</sup> on the top, 5 mA/cm<sup>2</sup> in the middle and 10 mA/cm<sup>2</sup> on the bottom row.

Figure 8 presents graphically the values gathered in Table 5. On the vertical axis, the threshold stress derived for each one of the 12 scenarios studied (4 materials × 3 environments) applying ASTM F1624 is represented in a X-Y dispersion graph, related to its homologous threshold SPT load obtained by the proposed methodology, displayed in the X axis. This is to say, σ<sub>th</sub> is plotted against its corresponding P<sub>th-SPT</sub> from Table 5, where a certain correlation is found between the two threshold parameters (SPT load and F1624 stress), indicating some dependency between them. The correlation proposed is just valid for the SPT specimen, punch and tools geometries employed in this work, which are the ones recommended by the European standard. Although small SPT specimen thickness variations are admitted because the proposed expression corrects it, it must be noted that a thickness as close as possible to 0.50 mm must be used, and in this work a specimen thickness was contained in the range 0.50 ± 0.01 mm in all the cases.

From the aforementioned previous works by the authors [7], in which the following model is explained in detail, given that the threshold stress obtained by both methods must be equal

$$\sigma_{th-ASTM} = \sigma_{th-SPT} = \sigma_{el-SPT} + \sigma_{pl-SPT} \rightarrow \sigma_{pl-SPT} = \sigma_{th-ASTM} - \sigma_{el-SPT} \quad (5)$$

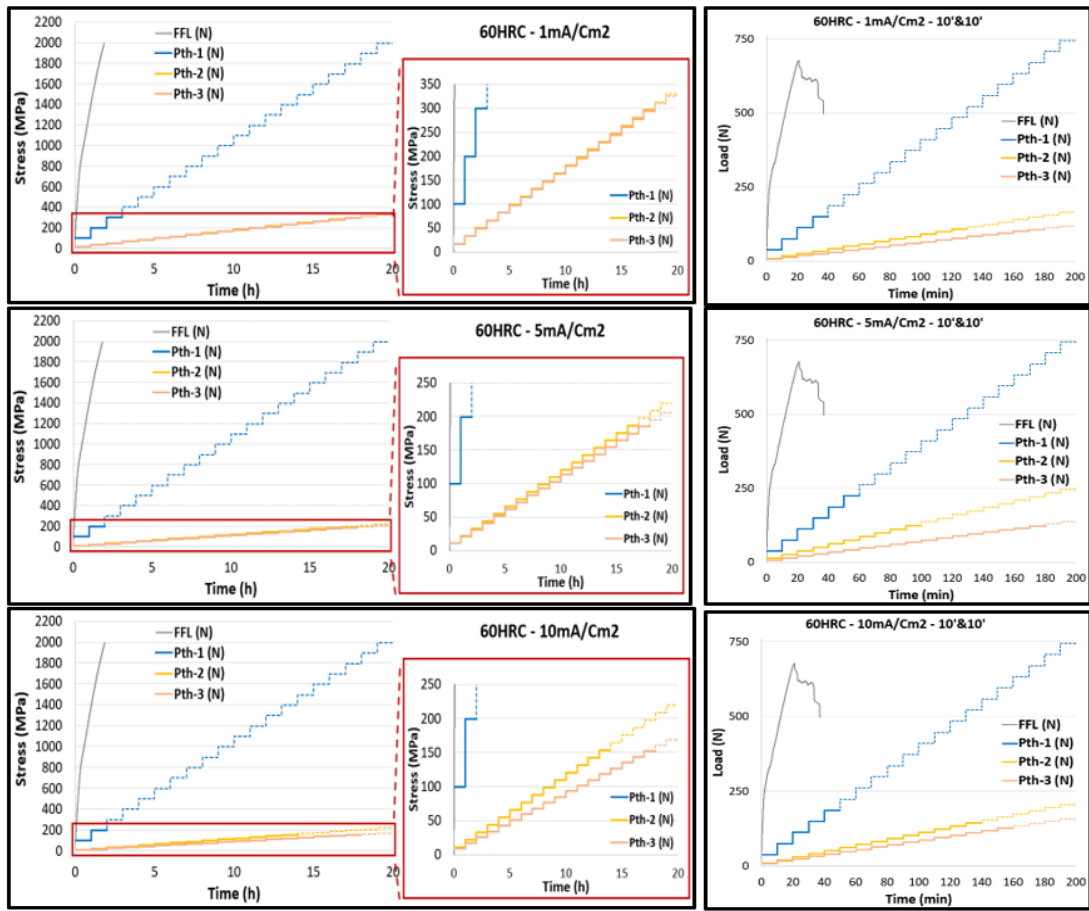


Figure 7. Threshold stress according to ASTM F1624 (left) and the corresponding threshold load values obtained with the proposed SPT method (right).

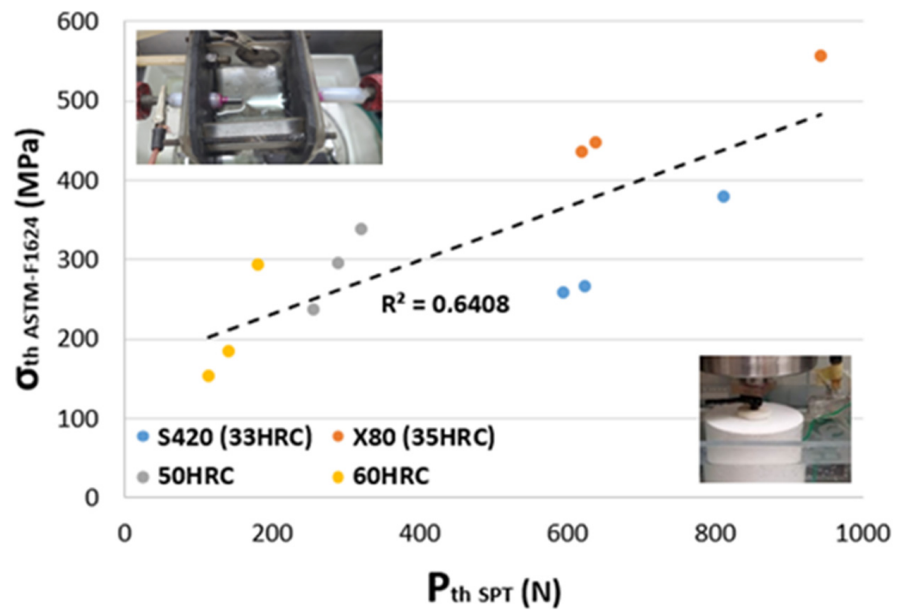
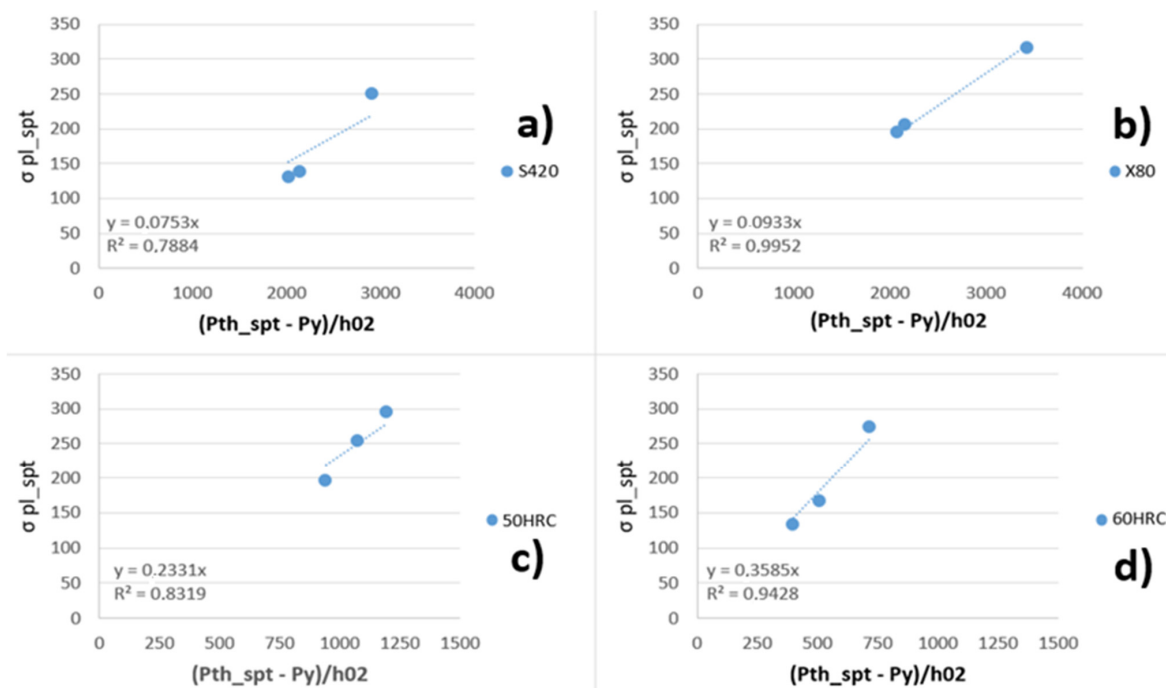


Figure 8. Correlation found between the SPT threshold load and the ASTM F1624 stress value in the various materials and stresses and environments under study.

And equating the plastic components from Equations (3) and (5)

$$\sigma_{th-ASTM} - \sigma_{el-SPT} = \frac{\alpha}{h_0^2} \cdot (P_{th-SPT} - P_y) \rightarrow \sigma_{pl-SPT} = \alpha \cdot \frac{(P_{th-SPT} - P_y)}{h_0^2} \quad (6)$$

In this plastic component, there is an  $\alpha$  coefficient that needs to be calibrated. This is performed for each one of the materials, as there is no reason to think that  $\alpha$  will be a constant value, having most probably a material and/or environmental dependence. As a result of this, it can be observed that a linear relationship that passes through the origin with a proper correlation coefficient ( $R^2$ ) can be established in all the cases, which means that there is a quasi-independence of the environment;  $\alpha$  can be calculated directly as the slope of the resulting line for each material, as can be observed in Figure 9. Analyzing the values obtained, different for each material, the material dependence of  $\alpha$  can be established.



**Figure 9.** Adjustment of the  $\alpha$  coefficient for the materials and the environments analyzed in this work: (a) S420; (b) X80; (c) 50 HRC; (d) 60 HRC.

Table 6 summarizes the values of  $\alpha$  obtained for each material, whereas Figure 10 plots the dependence of the parameter  $\alpha$  with the material hardness (HRC), which shows good trends. It must be pointed out that, as the ASTM F1624 methodology is just valid for steels of a hardness over 33 HRC, the SPT proposal has been validated in the same range, so it is just valid for those situations. The reason is that it is medium- and high-strength steels that mainly suffer environmental problems, so the step methodology has just been studied in those cases for a practical reason.

**Table 6.**  $\alpha$  coefficient value obtained with the model adjustment in the materials and environments studied.

Material (HRC)	Hardness (HRC)	$\alpha$
S420	33	0.0753
X80	35	0.0933
50 HRC	50	0.2331
60 HRC	60	0.3585

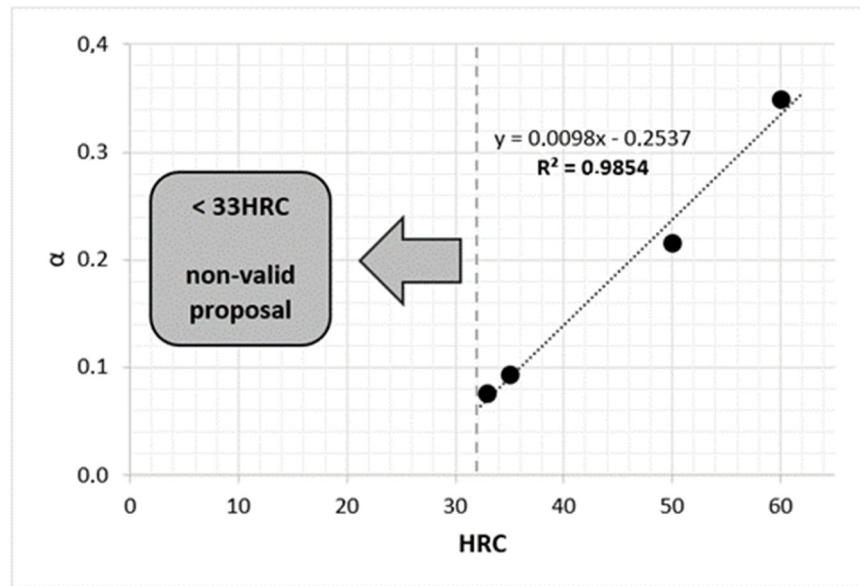


Figure 10. Correlation between  $\alpha$  coefficient and HRC hardness.

#### 4. Discussion

From the analysis of the presented results, the  $\alpha$  coefficient does not seem to depend on the environment. However,  $\alpha$  maintains a clear dependency on the material hardness in the range of materials and environments covered in this research, as has been shown in Table 6 and Figure 10.

By implementing the above-exposed dependency of the  $\alpha$  coefficient in equation (4), the threshold stress values may be easily estimated from the SPT threshold loads obtained in the Small Punch tests (Table 5). Figure 11 shows the comparison between the threshold values obtained from conventional tensile specimens and those derived from the SPT. It can be appreciated that the values are always contained within a  $\pm 10\%$  deviation, as is usual in SPT estimations.

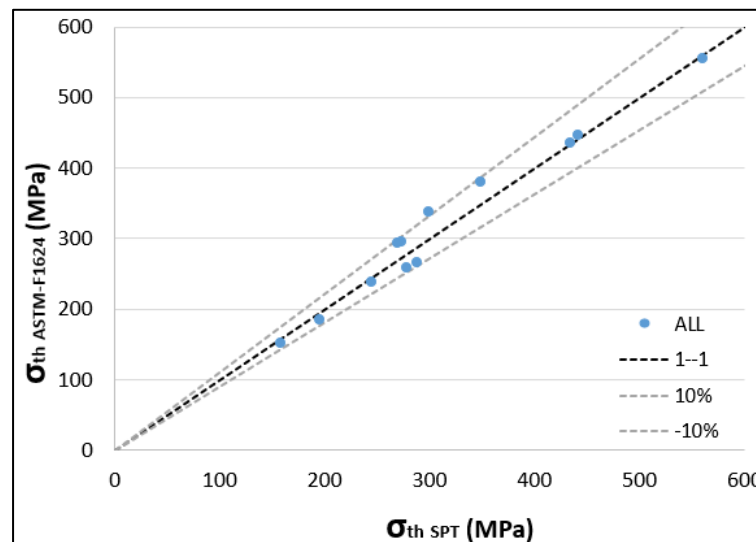


Figure 11. Proposed estimation of threshold stress based on SPT tests.

Similar correlations could be obtained with other hardness scales such as HV (Vickers) and HB (Brinell). However, ASTM F1624 works with HRC (Rockwell) and a conversion of units would be less operational without providing any additional advantage.

## 5. Conclusions

This paper provides a comprehensive validation of the model proposed by the authors, which allows the threshold stress defined by ASTM F1624 to be estimated from Small Punch tests results. The model consists of a correlation composed by an elastic and a plastic part, and it significantly reduces the time and material requirements of conventional tests. The validation provides a sound methodology to estimate the threshold stress in medium- and high-strength steels with a hardness above 33 HRC, up to at least 60 HRC.

Four materials and three levels of aggressiveness have been employed, incorporating the optimal step times defined in the literature, in order to calibrate the model for  $33 \leq \text{HRC} < 45$ ,  $45 \leq \text{HRC} < 55$  and  $\text{HRC} \geq 55$  ranges. However, these ranges, initially proposed in ASTM F1624 for conventional tests, could be unified for SPT tests if 20 and 40 minutes are used for the 1 to 10 and 11 to 20 steps in the whole range of hardness over 33 HRC (less time-efficient).

It has been proved that the elastic part only depends on the elastic-to-plastic transition SPT load ( $P_y$ ), while the plastic part is ruled by a material hardness-dependent coefficient. This coefficient has been found to be, in practice, independent of the environment, so the real dependences of the methodology come just from the material in terms of its hardness (by the calibrated coefficient  $\alpha$ ).

Future works should extend the proposed methodology to other environments and/or materials, in order to make the approach more robust if possible.

**Author Contributions:** Conceptualization, L.A. (Laura Andrea), B.A., J.A.Á. and F.G.-S.; methodology, B.A., L.A. (Laura Andrea), F.G.-S. and J.A.Á.; validation, L.A. (Laura Andrea), B.A., L.A. (Luis Abarca) and S.C.; formal analysis, S.C.; investigation, L.A. (Laura Andrea), B.A., J.A.Á., F.G.-S. and L.A. (Luis Abarca); resources, J.A.Á., B.A. and S.C.; data curation, L.A. (Laura Andrea), B.A. and L.A. (Luis Abarca); writing—original draft preparation, L.A. (Laura Andrea) and B.A.; writing—review and editing, B.A., S.C. and F.G.-S.; project administration, J.A.Á.; funding acquisition, J.A.Á. and B.A. All authors have read and agreed to the published version of the manuscript.

**Funding:** This research was partially funded by CONSEJERÍA DE EDUCACIÓN, FORMACIÓN PROFESIONAL Y UNIVERSIDADES DEL GOBIERNO DE CANTABRIA, Project DESARROLLO DE UNA METODOLOGÍA PARA EVALUAR LA INTEGRIDAD ESTRUCTURAL DE CORDONES DE ACERO PARA PRETENSADO DAÑADOS EN SERVICIO EN VISTA DE SU VIDA REMANENTE EN SERVICIO. (AYUDA FINANCIADA CONTRATO PROGRAMA GOB CANTABRIA-UC).

**Data Availability Statement:** The original contributions presented in the study are included in the article, further inquiries can be directed to the corresponding author/s.

**Conflicts of Interest:** The authors declare no conflicts of interest.

## References

1. ISO 7539, Parts 1 to 9; Corrosion of Metals and Alloys. ISO: Geneva, Switzerland, 2011.
2. ASTM E1681-03; Test Method for Determining Threshold Stress Intensity Factor for Environment Assisted Cracking of Metallic Materials. ASTM international: West Conshohocken, PA, USA, 2013.
3. ASTM F1624-18; Standard Test Method for Measurement of Hydrogen Embrittlement Threshold in Steel by the Incremental Step Loading Technique. ASTM International: West Conshohocken, PA, USA, 2018.
4. Zhu, X.; Peng, J.; Su, W.; Miao, X.; Ni, W.; Zhang, Q.; Zhang, R. Mechanical properties and fracture mechanism of CuCrZr alloy and pure Cu at high temperatures by small punch test. *J. Nucl. Mater.* **2024**, *601*, 155334. [[CrossRef](#)]
5. EN 10371:2021 E; Metallic Materials—Small Punch Test Method. European Standard, ICS 77.040.10. ICS: Marikina City, Philippines, 2021.
6. ASTM E3205-20; Standard Test Method for Small Punch Testing of Metallic Materials. ASTM International: West Conshohocken, PA, USA, 2020.
7. Arroyo, B.; Andrea, L.; Gutiérrez-Solana, F.; Álvarez, J.A.; González, P. Threshold stress estimation in hydrogen induced cracking by Small Punch tests based on the application of the incremental step loading technique. *Theor. Appl. Fract. Mech.* **2020**, *110*, 102839. [[CrossRef](#)]
8. Andrea, L.; Arroyo, B.; Álvarez, J.A.; Gutiérrez-Solana, F.; Cicero, F.; Guilbert, E. Optimization of Step Times for ASTM F1624 Methodology Applied to Small Punch Tests in Aggressive Environments. *Met. Index. J.* **2024**, *14*, 863. [[CrossRef](#)]
9. Specification API 5LD; Specification for CRA Clad or Lined Steel Pipe. American Petroleum Institute: Washington, DC, USA, 2009.

10. *BS EN 10225:2009*; Weldable Structural Steels for Fixed Offshore Structures Technical Delivery Conditions. British Standards Institution: London, UK, 2009.
11. Hamilton, J.M. The challenges of deep-water arctic development. *Int. J. Offshore Polar Eng.* **2011**, *21*, 241–247.
12. Wei, R.P. Hydrogen Effects in Metals. In *Thompson*; Bernstein, A.W., Ed.; AIME: New York, NY, USA, 1981; pp. 677–690.
13. Álvarez, J.A.; Gutiérrez-Solana, F. An elastic-plastic fracture mechanics based methodology to characterize cracking behaviour and its applications to environmental assisted processes. *Nucl. Eng. Des.* **1998**, *188*, 185–202. [[CrossRef](#)]
14. Bernstein, J.M.; Pressouyre, G.M. Role of traps in the microstructural control of hydrogen embrittlement of steels. *Noyes Publ.* **1988**, *74*.
15. *ASTM E-8*; Standard Test Methods for Tension Testing of Metallic Materials. ASTM Standards; ASTM International: West Conshohocken, PA, USA, 2004.
16. Arroyo, B.; Álvarez, J.A.; Gutiérrez-Solana, F.; Lacalle, R.; González, P. Rate effects on the estimation of fracture toughness by small punch tests in hydrogen embrittlement. *J. Strain Anal.* **2019**, *54*, 390–400. [[CrossRef](#)]
17. García, T.E.; Rodríguez, C.; Belzunce, F.J.; Peñuelas, I.; Arroyo, B. Development of a methodology to study the hydrogen embrittlement of steels by means of the small punch test. *Mater. Sci. Eng. A* **2015**, *626*, 342–351. [[CrossRef](#)]
18. Wang, Z.; Liu, H.; Watanabe, Y.; Shoji, T.; Zhong, X.; Li, Z.; Lozano-Perez, S. Diffusible hydrogen facilitated stress corrosion cracking in 316 stainless steel using in-situ gaseous hydrogen charging in simulated PWR environment. *Scr. Mater.* **2025**, *225*, 116390. [[CrossRef](#)]
19. Timoshenko, S.; Woinowsky-Krieger, S. *Theory of Plates and Shells*. McGraw Hill: New York, NY, USA, 1950.

**Disclaimer/Publisher’s Note:** The statements, opinions and data contained in all publications are solely those of the individual author(s) and contributor(s) and not of MDPI and/or the editor(s). MDPI and/or the editor(s) disclaim responsibility for any injury to people or property resulting from any ideas, methods, instructions or products referred to in the content.